Microelectronics Reliability 55 (2015) 2671–2677

Contents lists available at ScienceDirect

Microelectronics Reliability

journal homepage: www.elsevier.com/locate/mr

Failure-mechanism analysis for vertical high-power LEDs under external pressure

Guanggao Chen [a,b], Xiaokang Liu [a], Zongtao Li [a,b], Yong Tang [a], Longsheng Lu [a,*], Binhai Yu [a], Qiu Chen [a]

[a] Key Laboratory of Surface Functional Structure Manufacturing of Guangdong High Education Institutes, South China University of Technology, Guangdong, China
[b] Research and Development Center, Foshan, Nationstar Optoelectronics Co., Ltd, Guangdong, China

ARTICLE INFO

Article history:
Received 30 March 2015
Received in revised form 5 July 2015
Accepted 19 August 2015
Available online 26 September 2015

Keywords:
High-power LEDs
Mechanical strength
Failure mechanism

ABSTRACT

This paper presents the factors that have the greatest influence on the mechanical strength of high-power LEDs, including bonding wire modes, pressure angles, and falling speeds of the indenter. Results show that the LED strength is greatly impacted by the wire bonding modes. Two main failure modes are identified: the silicone-lens crack caused by the stress concentration and the open-circuit failure induced by fractures in the bonding wire. The fractures are all located at the top of the LED chip bond pad. The bonding wire fractures are localized in a necking in the heat-affected zone (HAZ) or formed along the edge of bonds. It is confirmed that the wire bonding modes impact the mechanical strength of the vertical LEDs. It is hoped that the findings of our work will guide further work to determine and improve the modes of bonding wires, as well as the LED installation.

1. Introduction

High-power LEDs are currently undergoing rapid development due to their significant advantages, such as providing high brightness and having a long life while saving energy. Currently, LEDs are mainly used in general lighting applications such as in indoor and landscape lighting, backlighting and in outdoor full-color displays [1,2].

Undoubtedly, in terms of their features, LEDs exhibit a superiority that conventional incandescent lamps or fluorescent lamps cannot achieve. However, reliability issues are still a considerable problem that restricts their applicability. Previous literature has indicated that excess moisture and high temperatures may result in a decrease in the luminous efficacy or the open-circuit failure of GaN LEDs [3–6]. Many experiments have also indicated that the operating temperature is an important factor affecting the mechanical reliability of LEDs [7–9]. This is because stress appears in LEDs during thermal cycling in the presence of different expansion ratios for various materials, which leads to crystal defects and open-circuits as a result of bonding wire fractures [10]. In addition, a stress-lifetime model based on the Arrhenius equation [4], which explores the relationship between thermal stress and life time, has been widely acknowledged. The reliability of LEDs has been greatly improved on the basis of this model [11].

Nevertheless, for solid-state lighting products to be successful, the best and brightest LEDs required should be available on the market. Moreover, the knowledge and support to handle these components in high-speed applications, that require high yields and low defect rates without damage to the LEDs, is also critical [12]. Notably, there are many external compressive loads that lead to LED failure, which causes uncertainties for engineers and impedes large-scale application of LEDs. Firstly, some LED packaging companies, including the CREE, have found that the catastrophic failure of LEDs with ceramic substrate may occur as a esult of improper parameter settings during the pick-and-place operation performed by the pick nozzles during the surface mounting process. Additionally, to meet the demands of specific illumination distributions, a secondary lens is used in high bay lights. Such a secondary lens may compress the LED as a result of inappropriate assembling, leading the LEDs lens to crack which can cause corrugation of the bonding wire.

At present, detailed investigations of LED failure issues under external pressure still focus on the chips, the silicone material and the bonding wires. For a cylindrical bonding wire with a circular crack, its stress intensity factor is given as:

$$K_I = \frac{P}{D^{3/2}}\left(1.72\frac{D}{d_0} - 1.27\right), \tag{1}$$

$$K_I \geq K_{IC}, \tag{2}$$

where: K_I is the stress intensity factor of the bonding wire; P is the drag force sustained by the bonding wire; D is the diameter of the bonding wire; d_0 is the diameter of the crack; and K_{IC} is the surface crack tenacity. As $K_I \geq K_{IC}$, the crack in the bonding wire continues to extend, finally resulting in fracture.

For silicone materials, various models have been proposed to study the deformation and the stress of viscous silicone under pressure. The model that has been proven to accurately predict the stress of

* Corresponding author at: Key Laboratory of Surface Functional Structure Manufacturing of Guangdong High Education Institutes, South China University of Technology, Guangdong, China.
E-mail address: meluls@scut.edu.cn (L. Lu).

http://dx.doi.org/10.1016/j.microrel.2015.08.008
0026-2714/

viscoelastic material during uniaxial compressive tests is related to this equation:

$$\sigma = \sqrt{3}\tau_0 \ln\left(2\sqrt{3}A_0\right) + \sqrt{3}\tau_0 \ln(\varepsilon), \quad (3)$$

where: τ_o is the initial-deviatoric stress, A_o is the cross section area of the material, and ε is the strain of the viscoelastic material.

However, previous literature fails to recognize the importance of the modes of bonding the wires in LED packaging, especially in terms of influencing the mechanical strength of the LED. Consequently, we consider that there is an urgency to propose methods for evaluating and analyzing the mechanical strength of LEDs under external pressure.

In this paper, a series of experiments that evaluate the mechanical strength of the LEDs in the presence of external pressure are conducted. LEDs with various types of bonding wires, which are of industrial importance today, are fabricated as samples. In order to replicate the loading of LEDs in various applications, four indenters of various angles and three loading speeds are set as the variable parameters. The mechanisms of LED failure are analyzed through visual detection methods using an optical microscope, X-ray imaging, and a scanning electronic microscope. Our experimental findings are promising towards developing bonding wire modes with high mechanical strength for LED packaging.

2. Experiments

Vertical high-power GaN LEDs (of type 3535 type) were used in the experiments, as shown in Fig. 1. The LED is composed of an LED chip bonded with silver paste, a high-temperature co-sintered ceramic (HTCC) lead frame substrate with top/bottom layer copper films, a bonding wire, and a dome-shaped silicone lens. The silicone is made using Dow Corning® OE-6650 resin with a weight ratio between the A:B components of 1:3. The diameter of the gold wire is 1 mil (25 μm). As shown in Fig. 2, the difference between the LEDs is the mode of bonding the wire. For the mode shown in Fig. 2(b), a gold ball is first bonded to the top of the chip and further stitched to the lead frame to form the tail bond, namely the C–L bonding wire. For the mode shown in Fig. 2(c), a gold ball is first bonded to the lead frame and then stitched to the top of the chip to form the tail bond, namely the L–B bonding wire. For the mode shown in Fig. 2(d), a single gold ball is bonded to the top of the chip first, then another gold ball is first bonded on the lead frame and then stitched to the top of the LED chip to form the tail bond, namely the BL–C bonding wire.

The experimental setup consists of driving, loading, and measurement modules, shown in Fig. 3. The driving module DC source to guarantee that the LEDs operate at a constant driving current of 350 mA. The loading module applies external pressure to the LEDs through indenters positioned at various angles. The measurement modules comprise a voltage measuring apparatus, a Myadvantech®4711A data acquisition system, and a force and displacement measuring sensor, which connect to a computer. In the external pressure setup, the LEDs are fixed horizontally by clamping to ensure that the wire-loop plane is initially vertical to the cusp lines of the five prismatic indenters. Also, the indenters are restricted to move downwards to compress the LEDs with various loading speeds until the LEDs are extinguished. The force sensor, which is connected to the indenter, records the corresponding displacement and force. The voltage detection and force detection are synchronized. Additionally, all pressure tests are conducted with at least three specimens to confirm the accuracy of the results. It is of course expected that there will be an acceptable error related to the force sensor in the tests, as well as various sections of no-load pressure displacement.

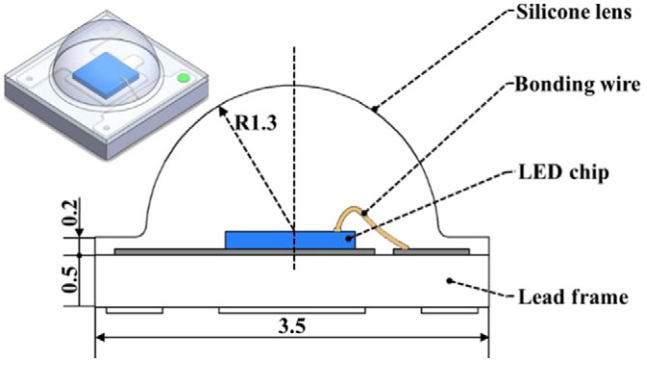

Fig. 1. The schematic of vertical structure 3535 LEDs.

It is known that LEDs can be submitted to external pressure by some applications and in the process of assembling backlight modules. In order to be able to study the mechanical strength of LEDs with three different types of bonding wire under external pressure, four indenters of different angles (30°, 90°, 150°, 180°) and three loading speeds (0.5 mm/min, 5 mm/min, 10 mm/min) are utilized in the experiments. Also, the indenter is made of steel, which has a much higher stiffness than the silicone lens.

3. Results and discussion

3.1. Failure force of LEDs in external pressure tests

During the experiments, a LED failure is defined as appearing when the LED cannot function normally anymore. The failure forces for LEDs using the three types of bonding wire that are mentioned in this paper, under external pressure, are shown in Fig. 4. The results demonstrate that the LED failure forces increase with loading speed i.e. the maximal failure forces appear at 10 mm/min loading speed. Additionally, the maximal failure forces of the C–L, L–B, BL–C LEDs are 56.3 N, 33.6 N, 33.7 N, respectively. As the angles of the indenters are increased, the failure forces of the C–L LEDs keep rising, while the other two types show a rise in failure forces followed by a decrease with a final increase. This is further discussed in the following sections.

For the C–L LED, the failure forces under pressure from the 30° and the 90° indenters are almost the same as the other two types, while the failure forces for the LEDs are much larger under pressure from the 150° and the 180° indenters than that of the other two types. For the L–B LEDs, the failure forces when using the 150° and 180° indenters are smaller than those under pressure from the 30° and 90° indenters. Finally, for the BL–C LEDs, the failure forces are slightly smaller than the forces of the L–B bonding wire under pressure applied with the 150° and 180° indenters.

Fig. 4 also shows that the LED exhibits a higher failure force as the loading speed rises, which corresponds to the LED sustaining a faster hit during assembly and application. This is because the faster the loading speed is, the higher the stress response amplitude of the silicone appears to be. As a result, C–L LEDs have the strongest mechanical strength. This is the reason why the C–L bonding wire is the dominant LED packaging technology in the industry. Hence, the following discussions are focused on the applied force response to displacement for LEDs using the C–L bonding wire.

The behavior of force-displacement for the indenter for C–L LEDs under external pressure is measured in the experiments, as shown in Fig. 5. When exposed to external pressure, the lens deforms. In the case of the 30° and 90° indenters, the pressure force firstly increases until it reaches a maximum, then drops dramatically, and finally starts rising again as the LEDs are forced to deform. At the end of the experiments, the silicone lens fractures can be observed in the optical images, as shown in Fig. 5. The point of fracture is defined by a sudden drop in force, which agrees with the results of fractures in the skin caused by labrum [13]. After a fracture appears, the LED continues to emit light

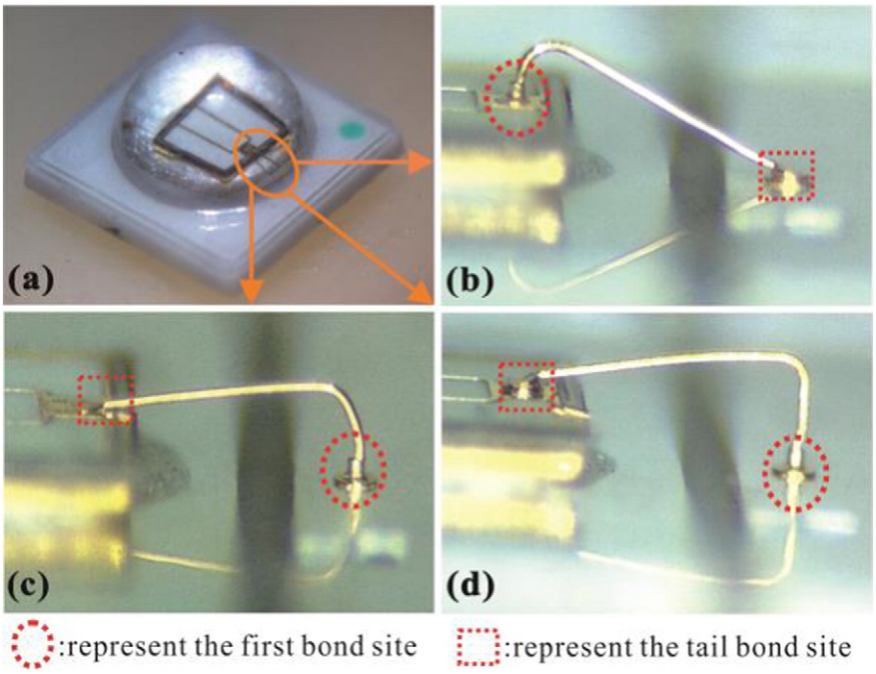

Fig. 2. Illustrations of LEDs with various bonding wires. (a) Axonometric view of LEDs; (b) profile view of C–L LEDs; (c) profile view of L–B LEDs; (d) profile view of BL–C LEDs.

normally at 3.2 V. However, the applied force may dramatically drop. It can be inferred that the LED electrical connections have not been damaged although the silicone lens appears to be cracked. After the forces drop to a minimum, it keeps rising, while the working voltage dramatically drops to almost 0 V. This is because the steel indenters have finally made contact with the LED chip, leading to short circuits. Meanwhile, the failure forces under the indenter with the 30° angle are smaller than those for the indenter with the 90° angle. This is because increasing the angle of the indenter leads to an increase in the distribution area of the applied force, resulting in lower stress. Furthermore, previous research has demonstrated that the fracture force of the viscoelastic material increases with the full cross-sectional area of the indenters [14].

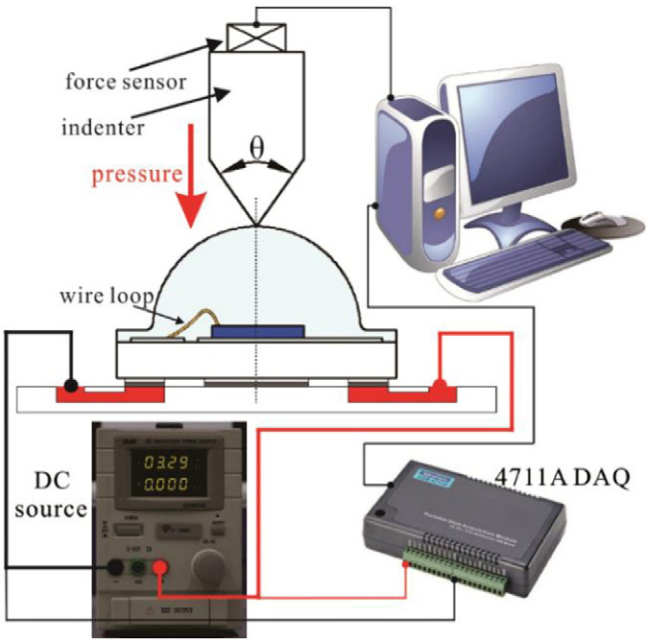

Fig. 3. Schematic of the experimental setup.

In the case of the 150° and 180° indenters, the pressure force keeps rising as the tip displacement increases, which means that the silicone lens does not crack. However, the electrical connections of the LEDs are damaged during this process, because their functional voltages jump to open-circuit voltages, and this is defined as open-circuit failure of the LEDs. The failure forces in the 180° indenter case are larger than those in the 150° indenter case; so it can be inferred that the open-circuit failure is mainly caused by the pressure tangential to the horizontal plane. Meanwhile, the results show that for the same indenter, the failure force keeps increasing as the loading speeds rise. According to results, there is a strong positive correlation between stress and strain rate. Obviously, when the LEDs are under external pressure, the larger loading speed results in a larger strain rate. Eventually, this leads to a larger pressure force. The results conform to the mechanical property of silicone in the uniaxial compressive test and are confirmed by Eq. (3). The shortcoming of the experiments is that there are different sections of no-load pressure displacement. This is the main reason that there are no clear consequences of displacement when LEDs suffer failure, even though the forces are highly repeatable.

In summary, it can be stated that there are two main failure modes: silicone lens fracture when pressure is applied via the 30° or 90° indenters and open-circuit failure when pressure is applied via the 150° or 180° indenters. The silicone lens failure is caused by a severe stress concentration corresponding to the sharp angle of the indenters. This is why tweezers are prohibited for delivery of LEDs during manufacturing. In industry, open-circuit failure in LEDs always causes confusion for engineers, and is also the main obstacle to general application of LEDs. The next section focuses on the open-circuit failure mechanism of LEDs.

3.2. Open-circuit failure analysis

In this section, X-ray and SEM images are used to analyze the open-circuit failure mechanism of LEDs. The C–L LEDs which suffer failure were characterized using X-ray imaging. For comparison purposes, the L–B, BL–C LEDs were also characterized, as shown in Fig. 6.

Notably, all breaks in the bonding wire are near the bonding pad at the top of the LED chips. Specifically, the fracture positions for the C–L LEDs are at the neck of the heat-affected zone (HAZ), shown in Fig. 6(a), while the positions are at the tail bond for the other two

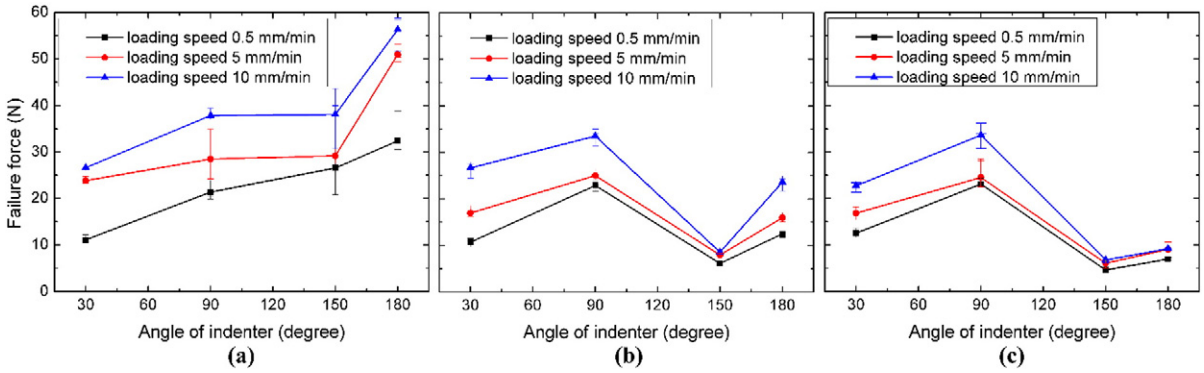

Fig. 4. The failure force of LEDs under pressure (a) C–L LEDs; (b) L–B LEDs; (c) BL–C LEDs.

types, shown in Fig. 6(b) and (c). The first bond and tail bond are both points of the bonding wire that have weak mechanical strength. It can be inferred that the deformation in the pad at the top of the LED is larger than that in the lead frame. In addition, for the LEDs using a C–L bonding wire, the HAZ in the bonding wire is near the top of the bonding pad in the chip. In the HAZ, the main fracture mechanism is the ball bonding; the electrical induced grain grow and then form equal-diameter grains, which leads to weak mechanical properties [15]. Thus, in HAZ, the neck, which is obviously affected by the stress concentration, is more likely to be the fracture position. To accomplish the formation of the tail bond, the gold wire deforms plastically and tears away. Mechanical hardening occurs in the tail bond, resulting in an increase in brittleness and in the risk of fracture.

To investigate the reason that open-circuit failure occurs when the LEDs are under pressure from the 150° or 180° indenter but not from the 30° or 90° indenter, the deformation of the bonding wire and lens for the same pressure displacement was detected, which is presented in Fig. 7. It is clear that the vertical variance of the lens volume (VVLV) increases as the angle of the indenter increases, the result being that silicone lens experiences greater expansion in the horizontal direction, since the volume of silicone is almost unchanged under pressure. The VVLV is larger when the LEDs are under pressure from the 150° or 180° indenter than from the 30° or 90° indenter, which leads the silicone lens to expand dramatically in the horizontal direction, resulting in a fracture of the bonding wire. However, the lens does not crack as there is a lower stress concentration in the lens.

To figure out the reason for the differences in failure forces for LEDs using the three types of bonding wire under external pressure, the silicone lens is firstly removed by application of a hot lytic agent and then the fracture positions of the bonding wires are observed through SEM, as shown in Fig. 8.

Fig. 8(a) presents a necking in the fracture of the C–L bonding wire. It shows that the slip lines were close to the bonds and to the wire fracture [16]. Also, the fracture site is near the columnar grains, because the

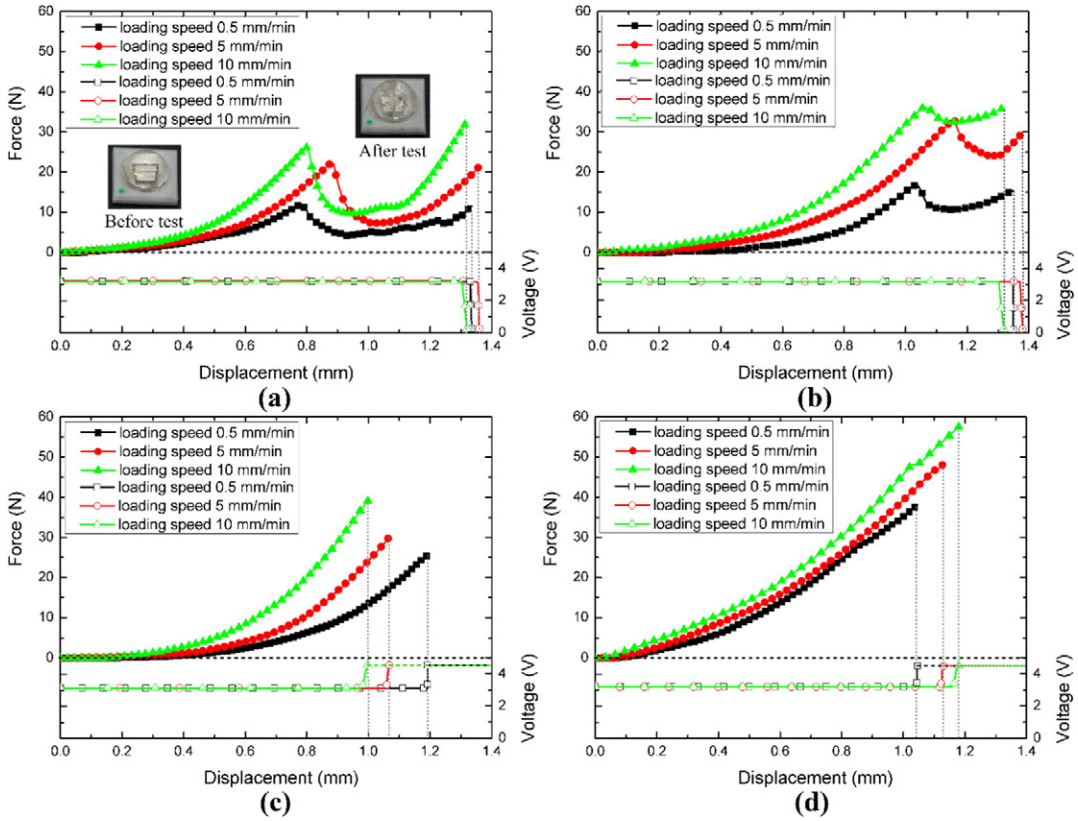

Fig. 5. The experimental pressure force of LEDs for various indenters and loading speeds (a) 30° indenter; (b) 90° indenter; (c) 150° indenter; (d) 180° indenter.

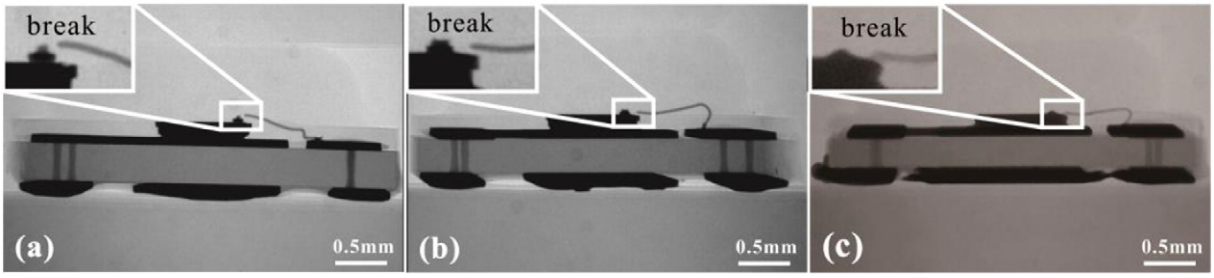

Fig. 6. The X-ray images of failure LEDs after external pressure tests (a) LEDs with C–L bonding wire; (b) LEDs with L–B bonding wire; (c) LEDs with BL–C bonding wire.

columnar grains have a higher deformation resistance [17]. Additionally, the direction of the slip lines is tangential to the horizontal plane, which may indicate that the C–L bonding wire is mainly cut off by the shear stress. For L–B, BL–C bonding wires, their fractures were formed along the edge of the bonding spots [18], as shown in the Fig. 8(b) and (c). Obviously, the orientation of the fractures is not coincident with the vertical plane. Moreover, it is observed that the fracture site is close to the bonding site fixed by the bonding pad on the LED chip. This may indicate that the L–B and BL–C bonding wires were mainly cut off by the horizontal drag force.

To confirm this inference, the deformation process was detected by X-ray and the fractures of the C–L bonding wire were focused on using SEM, as shown as Fig. 9. The X-ray images show that the sweep does not appear in the bonding wire while the LED is under pressure. In order to separate the influence of the bonding wire sag and that of the horizontal drag, Fig. 8(a) shows the bonding wire sag force F_{sag} and horizontal drag force F_{drag} caused by the deformation of the silicone lens during the LED pressurization. Fig. 9(a), (b), (c) present the process, showing how the bonding wire deforms and eventually fractures while the LED is under pressure from the 180° indenter. It can be deduced that the B–L bonding wire appears to be slightly sagging, which is mainly caused by the sag force F_{sag}. Notably, the bonding wire around the fracture site dislocates horizontally. The isometric of the fracture site is shown in Fig. 9(d). The slip plane is almost horizontal and differs from the slip plane of the fracture caused by the pull test [16]. To summarize, a study of the LEDs under pressure from the 180° indenter shows that the fracture is characterized by a horizontal slip plane caused by the horizontal force, which is the main reason for the open-circuit failure mechanism.

Compared to the C–L bonding wires, the sectional areas in the fracture position of the L–B and BL–C bonding wires are much smaller, which means that severe stress concentration is more likely. Thus, the failure forces for the LEDs with the L–B and BL–C bonding wires are much smaller than those of the LEDs with the C–L bonding wire when the LEDs suffer open-circuit failure under external pressure. In regards to the silicone lens on the surface of LED chips under external pressure, the deformation becomes larger as the distance from the surface of the chip increases. This indicates that the failure forces for L–B LEDs are slightly higher than those for the BL–C bonding wires. Based on these findings, we recommend that LEDs using C–L bonding wires should be in widespread use in industry, and call for more attention in this area in order to avoid wire fractures in the bond pad on the top of the LED chip.

4. Conclusions

We have analyzed the mechanical failures of high-power LEDs through external pressure tests. Although precision may be limited due to the limited set of test samples, the technique can still serve to provide guidelines for further research on the deformation process of

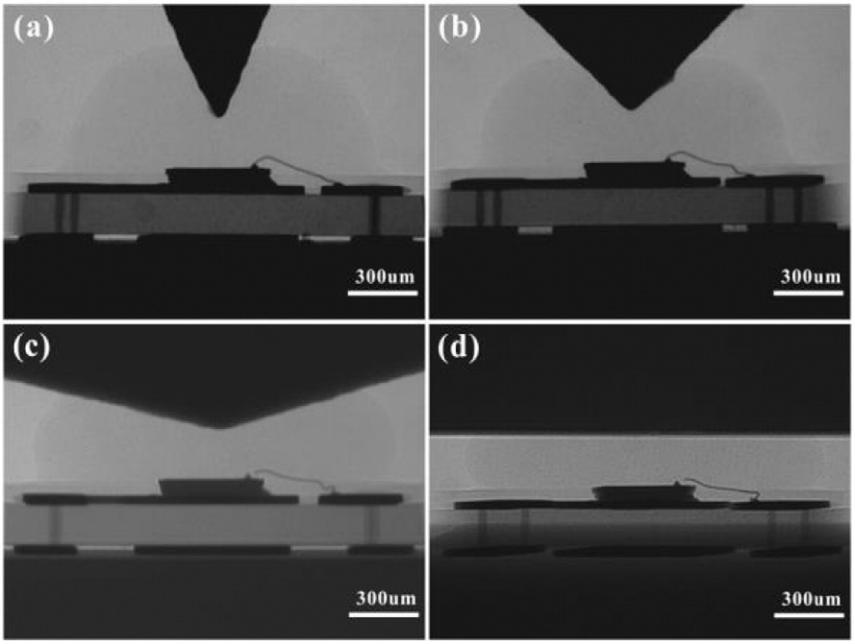

Fig. 7. The deformation of bonding wire and lens in C–L LEDs during pressuring for various indenters (a) 30° indenter; (b) 90° indenter; (c) 150° indenter; (d) 180° indenter.

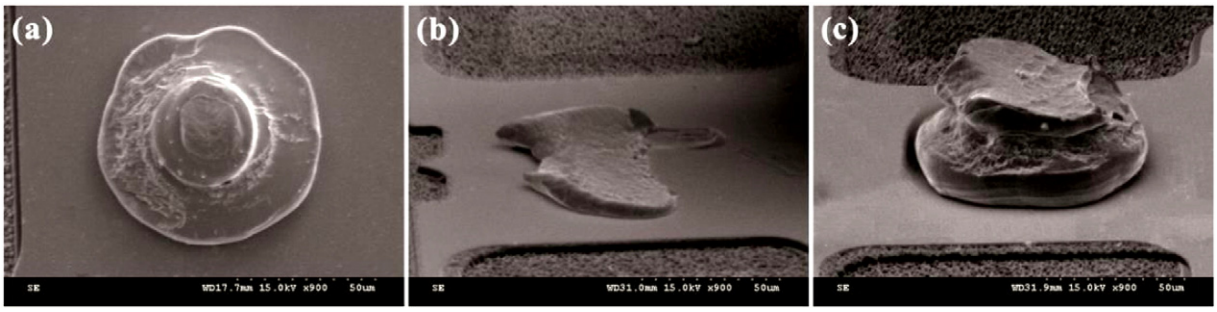

Fig. 8. The SEM photographs of fracture observation of three kinds of LEDs (a) C–L LEDs; (b) L–B LEDs; (c) BL–C LEDs.

silicone lenses and the rigidity of the silicone lens. The failure forces of LEDs have been discussed and the failure mechanisms analyzed through use of an optical microscope, X-ray images, and SEM. The main conclusions of these tests are as follows:

1. In the external pressure tests, there are two failure modes: silicone lens cracks and open-circuit failure. When the LEDs are under pressure from the 30° or 90° indenters, they may suffer from a silicone lens crack because of the stress concentration, while under pressure from the 150° or 180° indenters, they may suffer from open-circuit failure because of a break induced in the bonding wire.
2. The failure forces are almost the same when the LEDs suffer a silicone lens crack. However, the failure forces for LEDs with the C–L bonding wire are much higher than the failure forces for the other two types when open-circuit failure occurs. The results show that the LEDs with the C–L bonding wire have the highest mechanical strength.
3. With respect to the open-circuit failure, the fractures in the bonding wire were observed by X-ray imaging. For the C–L bonding wire, the fracture position is within the heat-affected zone, while for the L–B and BL–C bonding wires, their fracture positions are at the tail bonding. It can be inferred that the bonding pad at the top of the chip suffers from much larger deformation than the lead frame.
4. For the L–B and the BL–C bonding wires, their fractures are formed along the edge of the fixed bonding spots. For the C–L LEDs that suffer from open circuit failure, the bonding wires near the fracture are dislocated horizontally, and a slip plane is also formed horizontally to the fracture, indicating that the main mechanism of the fracture is produced by the horizontal drag force applied to the bonding wire. It can be inferred that open-circuit failure is caused mainly by the horizontal force.

Acknowledgments

This work is supported by the National High-Tech R&D Program of China (863 Program), No. 2013AA03A110, the National Natural Science Foundation of China, No. U1401249 and No. 51405161, as well as by the Postdoctoral Science Foundation of China, No. 2014M560659.

References

[1] M.-T. Lin, S.-P. Ying, M.-Y. Lin, K.-Y. Tai, J.-C. Chen, High power LED package with vertical structure, Microelectron. Reliab. 52 (2012) 878–883 (5//).
[2] S.R. Lee, C. Lau, S. Chan, K. Ma, M. Ng, Y. Ng, et al., Development and Prototyping of a HB-LED Array Module for Indoor Solid State Lighting, High Density Microsystem Design and Packaging and Component Failure Analysis, 2006. HDP'06. Conference on 2006, pp. 141–145.
[3] L. Trevisanello, M. Meneghini, G. Mura, M. Vanzi, M. Pavesi, G. Meneghesso, et al., Accelerated life test of high brightness light emitting diodes, IEEE Trans. Device Mater. Reliab. 8 (2008) 304–311.
[4] J. Kim, B. Ma, K. Lee, Comparison of effect of epoxy and silicone adhesive on the lifetime of plastic LED package, Electron. Mater. Lett. 9 (2013) 429–432 (2013/07/01).

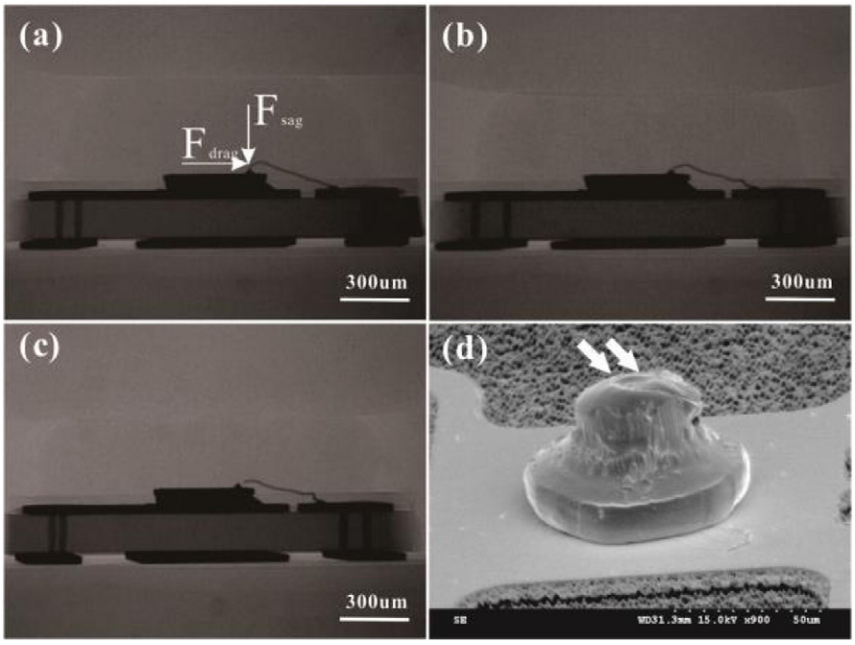

Fig. 9. The process of C–L LEDs being pressured by 180° indenter: (a) the LED was just attached by the indenter; (b) the bonding wire deformed but not cracked; (c) the LED having suffered open-circuit failure; (d) axonometric view of the slip plane at the fracture site.

[5] L. Xiaobing, W. Bulong, L. Sheng, Effects of moist environments on LED module reliability, IEEE Trans. Device Mater. Reliab. 10 (2010) 182–186.
[6] P. Lall, H. Zhang, Assessment of lumen degradation and remaining life of light-emitting diodes using physics-based indicators and particle filter, J. Electron. Packag. 137 (2015) 021002.
[7] M.-H. Chang, D. Das, P.V. Varde, M. Pecht, Light emitting diodes reliability review, Microelectron. Reliab. 52 (2012) 762–782 (5//).
[8] F. Wu, Z. Wei, Y. Shaohua, Z. Chunhua, Failure Modes and Failure Analysis of White LEDs, Electronic Measurement & Instruments, 2009. ICEMI '09. 9th International Conference on 2009, pp. 4-978–4-981.
[9] Z. Li, Y. Tang, X. Ding, C. Li, D. Yuan, Y. Lu, Reconstruction and thermal performance analysis of die-bonding filling states for high-power light-emitting diode devices, Appl. Therm. Eng. 65 (2014) 236–245.
[10] J. Tharian, Degradation-and failure mode analysis of III-V nitride devices, IPFA 2007. 14th International Symposium on the, 20072007.
[11] E. Nogueira, M. Vázquez, C. Algora, Accelerated life testing in epoxy packaged high luminosity light emitting diodes, J. Electron. Packag. 133 (2011), 034501.
[12] cree Xlamp pick and place Application note, www.cree.com/LED-Components-and-Modules/Document-Library.
[13] X. Kong, C. Wu, Measurement and prediction of insertion force for the mosquito fascicle penetrating into human skin, J. Bionic Eng. 6 (2009) 143–152.
[14] S.P. Davis, B.J. Landis, Z.H. Adams, M.G. Allen, M.R. Prausnitz, Insertion of microneedles into skin: measurement and prediction of insertion force and needle fracture force, J. Biomech. 37 (2004) 1155–1163.
[15] S. Murali, N. Srikanth, C.J. Vath III, Grains, deformation substructures, and slip bands observed in thermosonic copper ball bonding, Mater. Charact. 50 (2003) 39–50.
[16] I. Huang, F.-Y. Hung, T.-S. Lui, L.-H. Chen, H.-W. Hsueh, A study on the tensile fracture mechanism of 15 μm copper wire after EFO process, Microelectron. Reliab. 51 (2011) 25–29.
[17] F.-Y. Hung, T.-S. Lui, L.-H. Chen, Y.-C. Lin, Electric flame-off characteristics and fracture properties of 20. MU. M thin copper bonding wire, Mater. Trans. 50 (2009) 293–298.
[18] S. Murali, N. Srikanth, C.J. Vath, An evaluation of gold and copper wire bonds on shear and pull testing, J. Electron. Packag. 128 (2006) 192–201.